Magnetic Dimer Excitations in Cs3Cr2Cl9 Studied by Neutron Scattering

Leuenberger, Bruno; Güdel, Hans U.; Kjems, Jørgen; Petitgrand, Daniel; Brillouin, Leon

Published in:
Inorganic Chemistry

Link to article, DOI:
10.1021/ic00201a015

Publication date:
1985

Document Version
Publisher's PDF, also known as Version of record

is the photoproduct in this case), also demonstrated hydroxide ion quenching. Stern-Volmer plots of ϕ_p values vs. hydroxide concentration were linear, with K_{SV} values that approximated those from the emission experiments; however, experimental uncertainties were much larger owing to the small spectral changes monitored under these conditions ($\Delta\epsilon = -15$ at 305 nm). In strongly basic solutions, the photoreaction under 313-nm irradiation was completely quenched.

The above KIE for the hydroxide quenching of $[RhA_6^{3+}]^*$ and a similar one reported[7] (but not discussed) for the quenching of $[Rh(NH_3)_5Cl^{2+}]^*$ are comparable to the KIE of 1.77 ($k^H = 1.4 \times 10^{11}$ M^{-1} s^{-1}) reported[18] for the reaction of H^+ (D^+) with OH^- (OD^-) in H_2O (D_2O). This adds credence to the earlier proposal by Adamson and co-workers that such quenching occurs by a proton transfer from the coordinated ammine of the excited complex.[7] That the k_q values approach the diffusion limit (a diffusion limit of 1×10^{11} M^{-1} s^{-1} at 25 °C can be estimated for the encounter of a $M(NH_3)_6^{3+}$ ion with OH^- by using 4.4 Å as the distance of closest approach)[19] implies that the ammines of the excited-state complex are significantly more acidic than those of the ground-state complex ($pK_a > 14$).[20] For comparison, the second-order rate constants (25 °C) for the reaction of OH^- with the weak acids NH_4^+ ($pK_a = 9.25$)[21] and $Ru(NH_3)_6^{3+}$ ($pK_a = 12.4$)[19] have been reported as 3.4×10^{10} and 2×10^9 M^{-1} s^{-1}, respectively. The hexaammineruthenium(III) ion offers as especially interesting comparison, given the analogy between this ion's $(t_{2g})^5$ electronic configuration and the $(t_{2g})^5(e_g)^1$ configuration of the LF state of the hexaamminerhodium(III) ion.

In summary, measurement of the excited-state emission lifetimes of $Rh(NH_3)_6^{3+}$ and $Rh(ND_3)_6^{3+}$ in solution supports the conclusion that deuteration effects on photoreaction quantum yields can be attributed to perturbations of the nonradiative deactivation rates. Dynamic quenching of both photoaquation and photoemission by hydroxide further supports the view that both processes originate from the same state or an ensemble of equilibrated states. Lastly, the kinetic isotope effect of 1.5 seen in the k_q values supports the suggestion of reactive quenching by excited-state proton transfer from coordinated ammine.

Acknowledgment. This research was supported by a grant from the National Science Foundation to P.C.F. The rhodium used in these studies was provided on loan from Johnson Matthey, Inc.

Registry No. $Rh(NH_3)_6^{3+}$, 16786-63-3; D_2, 7782-39-0.

(18) (a) Bannister, J. J.; Gormally, J.; Holzwarth, J. F.; King, T. A. *Chem. Br.* **1984**, *20*, 227. (b) Ertl, G.; Gerischer, H. *Z. Elektrochem.* **1961**, *65*, 625. (c) Ertl, G.; Gerischer, H. *Z. Elektrochem.* **1962**, *66*, 580.
(19) (a) Waysbort, D.; Navon, G. *J. Phys. Chem.* **1973**, *77*, 960. (b) Waysbort, D.; Navon, G. *J. Chem. Soc. D* **1971**, 1410.
(20) Basolo, F.; Pearson, R. "Mechanisms of Inorganic Reactions"; Wiley: New York, 1967; p 33.
(21) Eigen, M.; Schoeu, J. *Z. Elektrochem.* **1955**, *59*, 483.

Contribution from the Institut für anorganische Chemie, Universität Bern, CH-3000 Bern 9, Switzerland, and Laboratoire Léon Brillouin, CEN Saclay, F-91191 Gif-Sur-Yvette, France

Magnetic Dimer Excitations in $Cs_3Cr_2Cl_9$ Studied by Neutron Scattering

BRUNO LEUENBERGER,*† HANS U. GÜDEL,*† JØRGEN K. KJEMS,†§ and DANIEL PETITGRAND‡

Received June 26, 1984

The energy dispersion of the singlet-triplet dimer excitation in $Cs_3Cr_2Cl_9$ has been studied by inelastic neutron scattering (INS) at temperatures down to 1.3 K. The results can be accounted for by using a completely isotropic Heisenberg Hamiltonian in the random phase approximation (RPA). Only nearest-neighbor interactions need to be considered. From the excellent fit, three exchange parameters were obtained: $J = -1.75$ meV (intradimer), $J_p = -0.032$ meV (interdimer, intrasublattice) and $J_c = -0.031$ meV (interdimer, intersublattice). These values indicate that $Cs_3Cr_2Cl_9$ is far from ordering magnetically. The systematic variation of the exchange parameters on substitution of Cl by Br and I is discussed.

Introduction

$Cs_3Cr_2Cl_9$ exemplifies a family of compounds in which the magnetic ions occur as dimeric complexes, $Cr_2Cl_9^{3-}$. The space group is hexagonal, $P6_3/mmc$, and there are two dimers per unit cell forming two sublattices.[1] A schematic structure is shown in Figure 1, indicating the two sublattices and the three exchange parameters. The Cr-Cr separation is 3.2 Å within the dimers and 7.2 Å (intrasublattice) and 7.1 Å (intersublattice) between nearest-neighbor dimers. There are Cr-Cl···Cl-Cr contacts between the dimers, providing pathways for weak interdimer interaction. The low-temperature magnetic and spectroscopic properties have so far been interpreted as resulting from isolated antiferromagnetically coupled dimers.[2-4] EPR spectra at elevated temperatures, where the first excited dimer level becomes populated, showed some evidence for interdimer exchange.[5] Previous inelastic neutron scattering (INS) experiments on $Cs_3Cr_2Cl_9$ indicated some interdimer interactions even at 1.8 K, where the dimer triplet population is negligible.[6] But the data in ref 6 were ambiguous due to the bad quality of the crystal. Here we report INS results on a high-quality crystal.

The antiferromagnetic intradimer exchange leads to a Landé splitting pattern with the singlet dimer state as ground state and the triplet as first excited state. Much effort has been devoted to the question of under what conditions a singlet ground-state system can order magnetically.[7-9] The present study was motivated by the interest in magnetic dimers and in singlet ground-state magnets. The closely related $Cs_3Cr_2Br_9$ has recently been studied by INS.[8,9] The singlet-triplet excitation was found to exhibit pronounced dispersion. It could be accounted for by using three exchange parameters corresponding to the interactions shown in Figure 1, the intradimer exchange J and the interdimer exchange between nearest neighbors J_p (intrasublattice) and J_c

†Universität Bern.
‡CEN Saclay.
§Permanent address: Risø National Laboratory, DK-4000 Roskilde, Denmark.

(1) Wessel, G. J.; Ijdo, D. J. W. *Acta Crystallogr.* **1957**, *10*, 466.
(2) Johnstone, I. W.; Maxwell, K. J.; Stevens, K. W. H. *J. Phys. C* **1981**, *14*, 1297.
(3) Briat, B.; Russel, M. F.; Rivoal, J. C.; Chapelle, J. P.; Kahn, O. *Mol. Phys.* **1977**, *34*, 1357.
(4) Kahn, O.; Briat, B. *Chem. Phys. Lett.* **1975**, *32*, 376.
(5) Beswick, J. R.; Dugdale, D. E. *J. Phys. C* **1973**, *6*, 3326.
(6) Stebler, A.; Güdel, H. U.; Furrer, A.; Kjems, J. *J. Appl. Phys.* **1982**, *53*, 1996.
(7) Fulde, P. "Handbook on the Physics and Chemistry of Rare Earths"; Gschneidner, K. A., Eyring, L., Eds.; North-Holland: Amsterdam, 1978; p 296.
(8) Furrer, A.; Güdel, H. U. *J. Magn. Magn. Mater.* **1979**, *14*, 256.
(9) Leuenberger, B.; Güdel, H. U.; Stebler, A.; Furrer, A.; Feile, R.; Kjems, J. K. *Phys. Rev. B: Condens. Matter* **1984**, *30*, 6300.

0020-1669/85/1324-1035$01.50/0

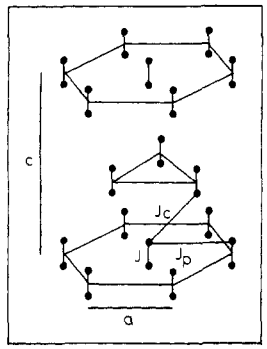

Figure 1. Schematic structure of $Cs_3Cr_2Cl_9$ indicating the three exchange parameters. The hexagonal lattice constants are a = 7.14 Å and c = 17.72 Å at 2 K. Only the Cr^{3+} ions are shown.

(intersublattice). The bromide is slightly undercritical; i.e., the interdimer exchange is almost strong enough to induce magnetic order. The substitution of Br by Cl is expected to increase the intradimer exchange, while the interdimer exchange is likely to decrease and thus reduce the tendency for magnetic order.

Experimental Section

Single crystals of $Cs_3Cr_2Cl_9$ were grown from stoichiometric mixtures of CsCl and $CrCl_3$ in quartz tubes at 900 °C by using the Bridgman technique. The crystals are fragile, soft, and air sensitive. For the neutron scattering experiments a single crystal of 2 cm^3 volume was mounted in an aluminum can under helium gas. All manipulations were performed in a glovebox under dry nitrogen or helium. The mosaic of the crystal was 0.8°.

INS experiments were carried out on the triple-axis spectrometer 4F1, which is located at the cold source of the reactor Orphée, CEN Saclay. A vertically focusing graphite (0, 0, 2) double monochromator was used, and a cooled beryllium filter was placed after the monochromator to eliminate higher order contaminations. The collimations were 60′–open–60′–40′–60′ along the path of the neutrons. The wave vector of the incident beam was fixed to 1.55 $Å^{-1}$, and scans were performed by varying the analyzer energy. The crystal was mounted in a pumped He cryostat with (0, 0, 1) and (1, 1, 0) lying in the scattering plane.

INS scans were obtained in the Γ-A (001) direction and the Γ-K-M (110) direction of the hexagonal lattice. The temperature was 1.3 K for the former and 2.6 K for the latter, but no influence of this temperature change was observed.

Results and Discussion

Transitions between the exchange-split levels of dimers of paramagnetic transition-metal ions can be observed by inelastic neutron scattering. In molecular systems with no or negligible interdimer exchange the excitations show no energy dispersion.[10] This is not true in $Cs_3Cr_2Cl_9$. Weak interdimer interactions lead to a dispersion of the singlet–triplet dimer excitation. Some selected INS scans of $Cs_3Cr_2Cl_9$ are shown in Figure 2. Well-defined peaks 5 observed, and the peak widths are due to the instrumental resolution. The peak positions evidently depend on the scattering vector, a quantity in reciprocal space. Figure 3 show the results of all the measurements.

We can interpret these results by applying a theory developed for $Cs_3Cr_2Br_9$, which was outlined in detail in ref 8. It will be summarized here. The following isotropic Hamiltonian can be written for $Cs_3Cr_2Cl_9$:

$$\mathcal{H} = -J\sum\vec{S}_{i1}\cdot\vec{S}_{i2} - \tfrac{1}{2}J_p\sum_{ij}(\vec{S}_{i1}\cdot\vec{S}_{j1} + \vec{S}_{i2}\cdot\vec{S}_{j2}) - \tfrac{1}{2}J_c\sum_{ij'}(\vec{S}_{i1}\cdot\vec{S}_{j'2} + \vec{S}_{i2}\cdot\vec{S}_{j'1}) \quad (1)$$

The double sums are restricted to nearest neighbors. By using the Green function method in the random phase approximation, we obtain two triply degenerate excitations:[8]

$$\omega^{ac,opt}(\vec{q}) = \{J^2 + M^2J(n_0 - n_1)(J_p\gamma_p(\vec{q}) \mp J_c|\gamma_c(\vec{q})|)\}^{1/2} \quad (2)$$

$M^2 = 5$ is the square of the singlet–triplet transition matrix element. The minus and plus signs correspond to the acoustic and optic modes, respectively. The singlet and triplet dimer states are populated according to the Boltzmann population factors n_0 and n_1. $\gamma_p(\vec{q})$ and $\gamma_c(\vec{q})$ are the Fourier sums over nearest-neighbor dimers within and between the sublattices. For the scattering law we obtain[8]

$$\frac{d^2\sigma}{d\Omega\, d\omega}(\vec{x},\omega) \approx F^2(\vec{x})\,(1 - e^{-\omega/kT})^{-1}(n_0 - n_1)(-J) \times (1 - \cos(\vec{x}\cdot\vec{R}))\left\{(1 + \cos(\vec{p}\cdot\vec{\tau} + \phi))\frac{1}{\omega^{ac}(\vec{q})}\delta(\omega - \omega^{ac}(\vec{q})) + (1 - \cos(\vec{p}\cdot\vec{\tau} + \phi))\frac{1}{\omega^{opt}(\vec{q})}\delta(\omega - \omega^{opt}(\vec{q}))\right\} \quad (3)$$

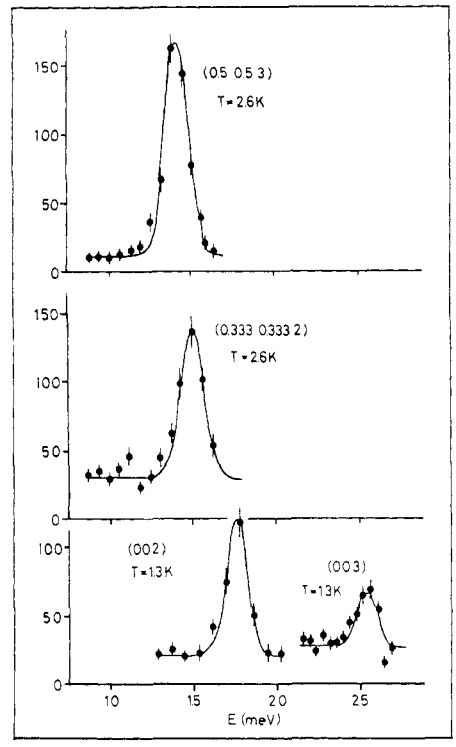

Figure 2. Selected INS scans illustrating the energy dispersion of the singlet–triplet excitation. The peak widths are resolution limited.

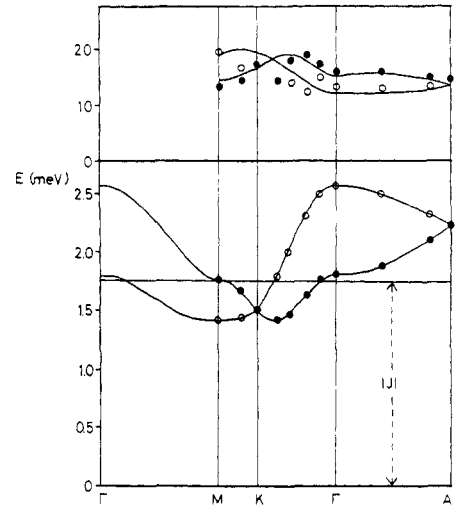

Figure 3. Singlet–triplet dispersion of $Cs_3Cr_2Cl_9$ in the three symmetry directions of the hexagonal lattice. The solid circles were measured from (0, 0, 2) to (0, 0, 2.5) and (0.5, 0.5, 2), while the open circles are in the zones (0, 0, 3) to (0, 0, 2.5) and (0.5, 0.5, 3). The lines correspond to a least-squares fit of eq 2 to the data. The lower curve is the acoustic and the upper the optic mode. Included are the calculated intensities and the observed integrated and corrected intensities as explained in the text.

(10) Leuenberger, B.; Güdel, H. U.; Feile, R.; Kjems, J. K. *Phys. Rev. B: Condens. Matter* **1983**, *28*, 5368.

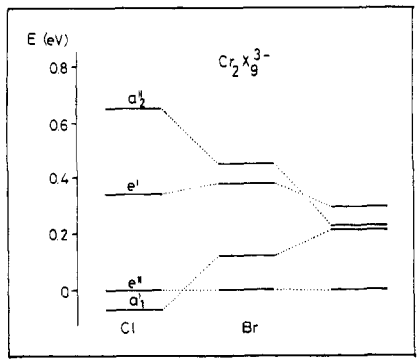

Figure 4. MO diagram of $Cr_2X_9^{3-}$ obtained from an extended Hückel calculation.[14] Only the relevant 3d part is shown. The point symmetry of the dimer is D_{3h}.

$F^2(\vec{x})$ is the square of the form factor of Cr^{3+}, $\vec{x} = \vec{\tau} + \vec{q}$ is the scattering vector, $\vec{\tau}$ a reciprocal lattice vector, $\vec{\rho}$ is α vector connecting the two sublattices, and R connects the two Cr^{3+} ions in a dimer. The Fourier sum $\gamma_c(\vec{q})$ is complex, and its phase is denoted by ϕ. On the basis of the factors $(1 \pm \cos(\vec{\rho}\cdot\vec{\tau} + \phi))$ we are able to distinguish acoustic and optic modes in our neutron spectra. From a least-squares fit to the observed energy dispersion we obtain the three exchange parameters

$$J = -1.75\ (1)\ \text{meV} \qquad J_p = -0.032\ (1)\ \text{meV}$$
$$J_c = -0.031\ (1)\ \text{meV} \tag{4}$$

The excellent fit is shown in Figure 3. Included in the figure is a comparison of the observed and calculated intensities. Since analyzer scans were done, the observed integrated intensities were approximately corrected for the instrumental resolution by the factor $k_f^3 \cot(\theta_A)$, where k_f is the final wave vector and θ_A the analyzer angle. The agreement between calculated and observed intensities is good.

If we compare the parameters[4] with those determined for $Cs_3Cr_2Br_9$,[8] we obtain ratios (chloride/bromide) of 1.706, 0.602, and 0.797 for J, J_p, and J_c, respectively. The reduction of the interdimer exchange compared to that for the bromide is related to the decrease of covalency when Br is substituted by Cl. This indicates that the interdimer exchange is due to superexchange pathways of the type Cr–X···X–Cr.

The increase of the intradimer exchange can be explained semiquantitatively within the framework of a simple mode.[11,12] The antiferromagnetic part of J is related to energy differences of molecular orbitals (MO) of the dimer built from atomic 3d orbitals:[13]

$$\frac{1}{2}J = -\frac{1}{9}\frac{1}{U}\left\{\frac{1}{2}(\epsilon_{a_1'} - \epsilon_{a_2''})^2 + (\epsilon_{e'} - \epsilon_{e''})^2\right\} \tag{5}$$

ϵ_i is the MO energy of the orbital of symmetry i, and U is the electron-transfer energy, which is considered to be independent of halogen type. The MO energies were obtained from an extended Hückel calculation.[14,15] The relevant part of the MO diagram for the chloride, bromide, and iodide is shown in Figure 4. It should be mentioned that this diagram has only semiquantitative character especially due to the small energy differences involved and the neglect of relativistic effects. Nevertheless, the diagram nicely explains the observed trend. Using the above formula, we obtain the ratio $J^{Cl}/J^{Br} = 1.8$, which, somewhat fortuitously, is in excellent agreement with the observed ratio of 1.71. From Figure 4 it is evident that the intradimer exchange

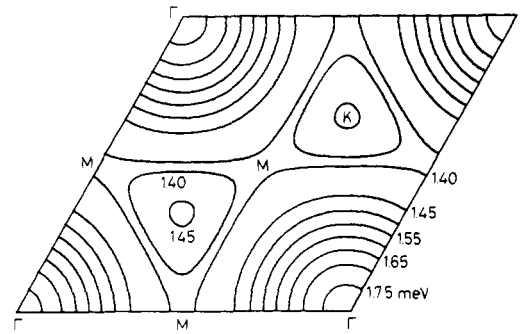

Figure 5. Energy contour plot of the acoustic mode.

Table I. Relevant Distances and Angles for the Interdimer Exchange Pathways J_p and J_c in the Compounds $Cs_3Cr_2X_9$

X	pathway	r(Cr–X), Å	Cr–X···X, deg	r(X···X), Å	"covalent part" of X···X, Å
Cl	J_p	2.44	131	3.93	
		2.27	137	3.80	0.25
	J_c	2.28	133	3.92	
		2.27	133	3.93	0.30
Br	J_p	2.56	132	4.05	
		2.40	137	3.95	0.08
	J_c	2.40	133	4.09	
		2.40	133	4.09	0.17
I	J_p	2.77	131	4.38	
		2.59	137	4.26	−0.08
	J_c	2.59	133	4.43	
		2.59	133	4.43	0.03

for the iodide is expected to be smaller than for the bromide, indicating that the ferromagnetic part of J, neglected in this discussion, could become important.

The ratio J_p/J_c, which is 1.3. for the bromide, is reduced to 1.05 for the chloride. as a consequence the minimum of the acoustic mode becomes more flat and less pronounced compared with that of the bromide and the M point is nearly a minimum point for the chloride, as can be seen from Figure 5. The change of this ratio must be related to small changes of the superexchange pathways. Neglecting the influence of the Cs^+ ions, we have to consider two exchange pathways for each of the interdimer interactions J_p and J_c. Relevant Cr–X and X···X distances as well as Cr–X···X angles are listed in Table I. The low-temperature structure parameters for the chloride and the bromide were determined by neutron diffraction.[16] For the iodide the lattice constants were obtained from a powder X-ray pattern and the scaled atomic positions of the bromide were used. No detailed structural information on the iodide is available at present. Therefore, this discussion contains some uncertainty as far as the iodide is concerned. It is interesting to note that all Cr–X···X angles in Table I are similar. In order to relate the X···X distances to exchange interactions, we subtract twice the x ionic raddii and thus obtain the "covalent part" of the X···X distance. This can then be used to predict the trend of the J_p/J_c ratio. Using ionic radii (Goldschmidt) of 1.81, 1.96, and 2.20 Å for Cl^-, Br^-, and I^-, respectively, and taking, for simplicity, the average X···X distance for a given interaction, we obtain the values listed in Table I. It is evident from these numbers that an increase of the J_p/J_c ratio is expected in the series chloride, bromide, iodide. This is in good agreement with the experimental values of 1.05 for the chloride and 1.39 for the bromide.

As a measure of the tendency for magnetic order in singlet ground-state systems, one often uses the ratio[7-9]

$$\left|\frac{M^2 J^*}{J}\right| \tag{6}$$

where $J^* = J_p\,\delta_p(\vec{q}_0) - J_c|\delta_c(\vec{q}_0)|$ at the minimum point $\vec{q}_0$ of the

(11) Hay, P. J.; Thibeault, J. C.; Hoffmann, R. *J. Am. Chem. Soc.* **1975**, *97*, 4884.
(12) Anderson, P. W. *Solid State Phys.* **1963**, *14*, 99.
(13) Leuenberger, B.; Güdel, H. U. *Mol. Phys.* **1984**, *51*, 1.
(14) Howell, J.; Rossi, A.; Wallace, D.; Haraki, K.; Hoffmann, R. *QCPE* **1977**, *5*, 344.
(15) Lohr, L. L.; Pyykkoö, P. *Chem. Phys. Lett.* **1979**, *62*, 333.
(16) Fischer, P., unpublished results.

acoustic mode. No transition to magnetic order is expected if this ratio is smaller than 1. For $Cs_3Cr_2Cl_9$ we obtain 0.36, whereas for $Cs_3Cr_2Br_9$ it is 0.92.[8] This shows that the chloride is far from ordering magnetically whereas the bromide is only slightly undercritical. In contrast the iodide is expected to order at finite temperature if it follows the above trend with a decrease of the intradimer exchange and an increase of the interdimer exchange compared to the bromide. We are currently investigating chemical and physical properties of the iodide.

Acknowledgment. This work was supported, in part, by the Swiss National Science Foundation and a NATO Senior Scientist Exchange Program.

Registry No. $Cs_3Cr_2Cl_9$, 21007-54-5.

Contribution from the Department of Chemistry,
Faculty of Science, Hokkaido University, Sapporo 060, Japan

Visible Absorption Spectral Studies of Molybdenum(V) Tetraphenylporphyrins in Organic Solvents

TAIRA IMAMURA,* TETSUYA TANAKA, and MASATOSHI FUJIMOTO*

Received April 18, 1984

Visible absorption spectra of molybdenum(V) tetraphenylporphyrin complexes, $Mo^VO(TPP)X$ (X = F, Cl, Br, NCS; TPP = *meso*-tetraphenylporphinato), in organic solvents and the substitution reactions of these complexes with dimethyl sulfoxide (Me_2SO) are discussed. The measurements of molecular weight revealed that these complexes exist as monomers in dichloromethane. Organic solvents used are classified as noncoordinating and coordinating solvents for these complexes. The shift of the main absorption bands, Soret, α, and β bands, of $Mo^VO(TPP)X$ in the noncoordinating solvents correlates with the function of refractive index, $(n^2 - 1)/(2n^2 + 1)$. The axial ligand X of these complexes is substituted by Me_2SO to form $[Mo^VO(TPP)\cdot Me_2SO]_s^+X^-$ in Me_2SO–CH_2Cl_2 via the solvated complex $[Mo^VO(TPP)X]_s$ as an intermediate. The values of the formation constants of $[Mo^VO(TPP)\cdot Me_2SO]_s^+X^-$ are in the order X = F $\ll$ NCS $\approx$ Cl $\ll$ Br.

Introduction

The reactions of molybdenum porphyrins in organic solvents are susceptible to influence from the impurities in solvents, air, and light. The complex $Mo^VO(TPP)OCH_3$ is formed immediately from $Mo^V(TPP)X$ (X = F, Cl, Br, NCS) in dichloromethane containing a trace amount of methanol[1] and reduced photochemically to $Mo^{IV}O(TPP)$.[2] The oxidation of $Mo^{IV}O(TPP)$ affords Mo(V) porphyrin complexes in the presence of anions or some impurities in organic solvents. In the γ-radiolytic reaction of $Mo^VO(TPP)X$[3] and the reaction of $Mo^VO(TPP)X$ with superoxide,[1,4] solvents also play a very important role. Therefore, we necessitated the study of the behavior of $Mo^VO(TPP)X$, in organic solvents.

There are many reports referring to the solvent effects on the behavior of metalloporphyrins in organic solvents.[5-15] However, the subjects of these studies are almost four-coordinated and five-coordinated metalloporphyrins with vacant sites at axial position. The present paper reports the studies of the visible absorption spectra of six-coordinated complexes $Mo^VO(TPP)X$ in various organic solvents and the substitution reactions of $Mo^VO(TPP)X$ with Me_2SO.

Table I. Molecular Weight of $Mo^VO(TPP)X$ in Dichloromethane at 31 °C

complex	mol wt	
	calcd	obsd
$Mo^VO(TPP)F$	743.73	759 ± 17
$Mo^VO(TPP)Cl$	760.18	771 ± 12
$Mo^VO(TPP)Br$	804.63	793 ± 14
$Mo^VO(TPP)NCS$	782.73	770 ± 14

Experimental Section

Materials. Dichloromethane, distilled, passed twice through a column of basic alumina, and dried over 4A molecular sieves overnight, was redistilled under Ar immediately before use. The purity of dichloromethane was checked spectrophotometrically by dissolving $Mo^VO(TPP)Br$. When the dichloromethane contains a trace of impurities such as alcohols, Cl^-, and some decomposed species as $CHCl_2^-$, the visible absorption spectra are changed by the formation of $Mo^VO(TPP)Cl$ or $Mo^VO(TPP)OR$.[16] Dimethyl sulfoxide was kept with calcium hydride for several days, distilled at 37 °C under reduced pressure, and stored under an Ar atmosphere. Other solvents were also carefully purified by usual methods. The complex $Mo^VO(TPP)X$ was synthesized by the method reported previously.[16]

Measurements. Visible absorption spectra were recorded with a Hitachi 808 spectrophotometer equipped with double-beam double monochromators at 25 ± 0.5 °C. The accuracy and reproducibility of the spectrophotometer are ±0.5 and ±0.2 nm, respectively. ESR spectra were recorded with a JEOL JES-FEIX spectrometer at 25 ± 2 °C. The molecular weight of $Mo^VO(TPP)X$ in dichloromethane was measured

(1) Imamura, T.; Hasegawa, K.; Tanaka, T.; Nakajima, W.; Fujimoto, M. *Bull. Chem. Soc. Jpn.* **1984**, *57*, 194.
(2) Ledon, H.; Bonnet, M. *J. Am. Chem. Soc.* **1981**, *103*, 6209.
(3) Imamura, T.; Takahashi, M.; Tanaka, T.; Jin, T.; Fujimoto, M.; Sawamura, S.; Katayama, M. *Inorg. Chem.* **1984**, *23*, 3752.
(4) Imamura, T.; Hasegawa, K.; Fujimoto, M. *Chem. Lett.* **1983**, 705.
(5) Nappa, M.; Valentine, J. S. *J. Am. Chem. Soc.* **1978**, *100*, 5075.
(6) Boucher, L. J. *Coord. Chem. Rev.* **1972**, *7*, 289.
(7) Hill, H. A. O.; Macfarlane, A. J.; Williams, R. J. *J. Chem. Soc. A* **1969**, 1704.
(8) Boucher, L. J. *J. Am.Chem. Soc.* **1968**, *90*, 6640.
(9) Corwin, A. H.; Chivvis, A. B.; Poor, R. W.; Whitten, D. G.; Baker, E. W. *J. Am. Chem. Soc.* **1968**, *90*, 6577.
(10) Whitten, D. G.; Baker, E. W.; Corwin, A. H. *J. Org. Chem.* **1963**, *28*, 2363.
(11) Kelley, S. L.; Kadish, K. M. *Inorg. Chem.* **1982**, *21*, 3631.
(12) Tsutsui, M.; Velapold, R. A.; Suzuki, K.; Vohwinkel, F.; Ichikawa, M.; Koyano, T. *J. Am. Chem. Soc.* **1969**, *91*, 6262.
(13) Kadish, K. M.; Shiue, L. R. *Inorg. Chem.* **1982**, *21*, 3623.
(14) Kadish, K. M.; Chang, D. *Inorg. Chem.* **1982**, *21*, 3614.
(15) Kadish, K. M.; Leggett, D. J.; Chang, D. *Inorg. Chem.* **1982**, *21*, 3618.
(16) Imamura, T.; Numatatsu, T.; Terui, M.; Fujimoto, M. *Bull. Chem. Soc. Jpn.* **1981**, *54*, 170.

0020-1669/85/1324-1038$01.50/0